

# Numeric Analyses of Dynamic Responses of Slope Based on Finite Element Method

**Atlas John**

Civil Engineering and Engineering Mechanics Department, Columbia University, USA

**E-mail:** [aj282@columbia.edu](mailto:aj282@columbia.edu)

## Abstract

The dynamic responses of slope on a saturated foundation are studied by using the nonlinear dynamic finite element method based on the plastic constitutive model, the influence of the saturated foundation upon the characteristics of dynamic pore pressure in foundation, seismic acceleration and deformation of slope is verified and analyzed. The results show that the dynamic pore pressure in the foundation increases larger and results in the foundation liquefaction, thus the slope large deformation caused by the foundation liquefaction have the great impact on the instability of slope during earthquake.

**Keywords:** Numeric Analyses, Dynamic Response, Finite Element Method, Earthquake.

## 1. Introduction

The instability of slope and the foundation liquefaction caused by earthquake are important research subjects in geotechnical earthquake engineering. Due to the technique complexity of dynamic centrifuge model test, currently, there is less experiment studied by using the arbitrary random wave on the seismic response of the slope on the saturated foundation, correspondingly there are less numerical simulation on analyzing the liquefaction problem and dynamic response of the slope on the saturated foundation by means of the elastic-plastic dynamic consolidation finite element method.

Arulanandan K used the sine wave as seismic input to carry out the dynamic centrifugal model test of a saturated slope under water level, and studied the slope failure phenomenon induced by liquefaction [1]. Yu and et al performed the dynamic centrifugal model test of a slope on the dry sand foundation by using the arbitrary random wave, and studied the dynamic response of dry sand slope [2]. Then Yu and et al carried out the dynamic centrifuge model tests of the slope on the saturated sand foundation using the arbitrary random wave, and studied the acceleration response of the slope, the changes of dynamic pore pressure and large deformation problem of the slope and the saturated sand foundation [3].

Currently, based on the Biot's dynamic coupled consolidation finite element method of two-phase saturated porous medium [4], the research of slope deformation and instability caused by foundation liquefaction is a key issue in geotechnical earthquake engineering. Zhang Hongyang and et al performed a comparison research on the seismic response of a shaking table test with the dynamic numerical simulation of a rockfill dam based on the generalized P-Z plastic model [5].

The mathematical generalized plasticity model is established and gradually developed to the Pastor-Zienkiewicz III model [6] and has a wide application [7]. This model belongs to a typical elastic-plastic dynamic constitutive model and has obvious advantages to simulate the seismic liquefaction of liquefiable soil, and can calculate the permanent deformation of soil, so it is one of the very practical constitutive to be applied in the analysis of soil deformation characteristics in the dynamic calculation. When the dynamic

computational analysis is used to evaluate the probability of liquefaction, the reasonableness and reliability of the computational result is mainly depended on the advanced characteristic of the adopted constitutive model and the reasonable parameters of constitutive model [8].

Based on the developed elastic-plastic dynamic consolidation analysis software FEMEPPDYN, aimed at the dynamic centrifugal model test of slope on the saturated sand foundation, this paper studied the acceleration response of slope, the dynamic pore pressure distribution of saturated sand foundation and slope large deformation caused by soil liquefaction in dynamic coupled consolidation numerical analysis, and analyzed the instability mechanism of slope.

## 2. The constitutive parameters of soil and validation of dynamic finite element software

### 2.1 The constitutive model and finite element program

The generalized plastic constitutive model of Pastor-ZienkiewiczIII totally needs 13 parameters, which can be obtained by the conventional triaxial compression test under the condition of the monotonic loading and the cyclic loading. The elastic relations are

$$\Delta \varepsilon_v^e = \frac{1}{K_{ev}} \Delta p' \quad (1)$$

$$\Delta \varepsilon_s^e = \frac{1}{G_{es}} \Delta q \quad (2)$$

with the elastic modulus

$$K_{ev} = K_{evo} \frac{p'}{p_0} \quad (3)$$

$$G_{es} = G_{eso} \frac{p'}{p_0} \quad (4)$$

where  $\Delta \varepsilon_v^e$  and  $\Delta \varepsilon_s^e$  are the elastic volumetric strain increments and the deviatoric strain increments,  $\Delta p'$  and  $\Delta q$  are the elastic volumetric stress increments and the deviatoric stress increments,  $K_{ev}$  and  $G_{es}$  are the elastic volumetric modulus and the shear modulus,  $p'$  is the mean effective stress,  $K_{evo}$ ,  $K_{eso}$  and  $p_0$  are parameters of constitutive model.

The loading direction  $\{\bar{n}\}$  is defined

$$\{\bar{n}\} = \frac{1}{\sqrt{1+d_f^2}} \left[ d_f \quad 1 \quad -\frac{1}{2} q M_f \cos 3\theta \right]^T \quad (5)$$

where  $q$  is the deviatoric stress,  $\theta$  is the Lode angle,  $d_f = (1+a_f)(M_f - \eta)$ ,  $\eta$  is the stress ratio,  $a_f$  is one of parameters of constitutive model,  $M_f$  is Lode angle dependent :

$$M_f = \frac{6M_{fc}}{6 + M_{fc}(1 - \sin 3\theta)} \quad (6)$$

where  $M_{fc}$  is one of parameters of constitutive model.

The plastic yielding function is defined :

$$f = q - M_f p' \left[ \frac{1+a_f}{a_f} \right] \left[ 1 - \left( \frac{p'}{p_c} \right)^a \right] \quad (7)$$

Corresponding plastic flow direction  $\{\bar{n}_g\}$  is

$$\{\bar{n}_g\} = \frac{1}{\sqrt{1+d_g^2}} \left[ d_g \quad 1 \quad -\frac{1}{2} q M_g \cos 3\theta \right]^T \quad (8)$$

where  $d_g$  is the dilatancy law,  $d_g = (1+a_g)(M_g - \eta)$ ,  $a_g$  is one of parameters of constitutive model,  $M_g$  is Lode angle dependent :

$$M_g = \frac{6M_{gc}}{6 + M_{gc}(1 - \sin 3\theta)} \quad (9)$$

where  $M_{gc}$  is one of parameters of constitutive model.

The plastic potential function is defined :

$$g = q - M_g p' \left( \frac{1+a_g}{a_g} \right) \left[ 1 - \left( \frac{p'}{p_c} \right)^{a_g} \right] \quad (10)$$

Chan developed the assistant SM2D program for simulation of the soil triaxial test, the specific determination method of model parameters is shown in literature [5]. Based on Zienkiewicz's dynamic consolidation finite element method and the Pastor-Zienkiewicz III model, coupled the dynamic consolidation with dynamic reaction, this paper developed the elastic-plastic dynamic consolidation analysis software FEMEPPDYN, which can calculate the vibration and the diffusion and dissipation of the pore water pressure in the whole process of vibration.

### 2.2 The validation of finite element

In order to use the dynamic centrifuge model test to verify the numerical program for liquefaction analysis, so this program verification test adopted VELACS Model No.1[5].

The horizontal saturated foundation in VELACS Model No.1 is 20cm in depth (corresponding to the prototype of saturated foundation in depth of 10.0 m), the laminar model box is used to simulate one-dimensional shear effect of infinite horizontal soil stratum, the relative density of soil sample of the sand is 40%, and the VELACS Model No.1 uses water as the pore fluid in the model test. Imposes the earthquake under the centrifugal acceleration of 50g condition, the arrangement of the measuring point in model test are shown in Figure 1, where LVDT1-LVDT6 are displacement sensors, AH1- AH5 are horizontal acceleration sensors, AV1-AV5 are the vertical acceleration sensors and P1-P8 are pore water pressure sensors.

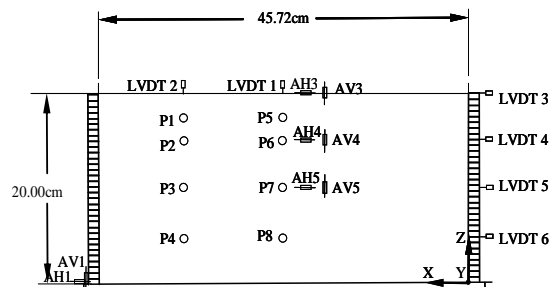


Fig.1 VELACS Model No.1

The solid grain density of Nevada sand is 2.67 g/cm<sup>3</sup>, the initial void ratio  $e$  is 0.736, and the corresponding model parameters of Pastor-Ziekiewicz III of Nevada sand are shown in Table 1.

In order to verify the FEMEPDYN software calculation function, the two-dimensional finite element model in shear effect mode (shown in Fig. 2) is established to simulate one-dimensional shear effect of infinite soil stratum. The boundary conditions of finite element model are as follows: (1) The bottom is treated as the acceleration input boundary. (2) The horizontal and vertical freedom degrees of nodes in the same elevation are same. (3) The pore water pressure in the surface nodes is zero. (4) The bottom and the side edge are impermeable boundary. The input of earthquake wave uses AH1 acceleration time history measured by VELACS Model No.1 (Fig. 3).

Table 1 Parameter of Pastor-Zienkiewicz III of Nevada sand [5]

Parameter	Value	Unit
$M_{fc}$	1.03	-
$M_{gc}$	1.15	-
$a_f \ a_g$	0.45	-
$K_{evo}$	770	kPa
$K_{eso}$	1155	kPa
$\beta_0$	4.2	-
$\beta_1$	0.2	-
$H_0$	600	-
$H_{u \ 0}$	4000	kPa
$\gamma$	0	-
$\gamma_u$	0	-
$p_0$	40	kPa

Through the calculation of elastic-plastic dynamic consideration analysis software FEMEPDYN, Fig. 4 shows the accelerometer AH3 in the centrifuge model test and the calculated time history of acceleration, it can be seen that the acceleration results are consistent in trend. Fig. 5 shows the time history of the excess pore pressure of the pore pressure gauge P7, the calculation results of excess pore pressure are more consistent in the accumulation and dissipation trend on the whole, and the dissipation of calculation results is lower.

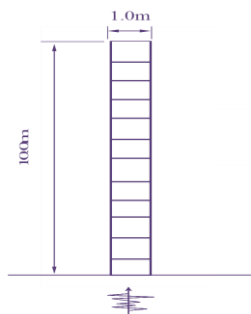


Fig.2 Finite element mesh

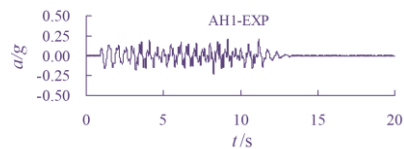


Fig.3 Input earthquake motion

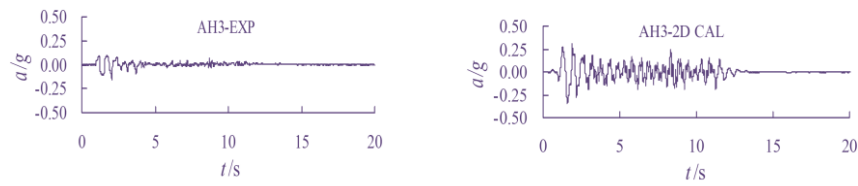


Fig.4 Acceleration AH3 history in experiment and computation



Fig.5 Response of pore pressure gauge P7 in test and calculation during earthquake

The comparison of the results in test with computation show that the program can perform the numerical analysis of the saturated soil liquefaction.

### 3. The computational analysis and discussion

The prototype slope on saturated foundation corresponding to the dynamic centrifuge model [3] is simulated and analyzed by the dynamic finite element method in this section. The parameters of Pastor-Zienkiewicz III of sand in BeiJing's White River are shown in Table 2.

Table 2 Parameter of Pastor-Zienkiewicz III of sand in BeiJing' White River

Parameter	Value	Unit
$M_{fc}$	0.95	-
$M_{gc}$	1.5	-
$a_f \ a_g$	0.45	-
$K_{evo}$	7440	(kPa)
$K_{eso}$	14150	(kPa)
$\beta_0$	1.0	-
$\beta_1$	0.1	-
$H_0$	700	-
$H_{u \ o}$	1000	(kPa)
$\gamma$	15	-
$\gamma_u$	20	-
$p_0$	100	(kPa)

The Fig.6 and Fig.7 are the arrangement of the accelerometer and the pore pressure sensors in the corresponding prototype slope. The three-dimensional finite element mesh is shown in Fig.8, the element employs the 8-node hexahedron, number of element is 559 and number of node is 1208. Boundary conditions of displacement: (1) the bottom is a fixed boundary; (2) the remote lateral boundary is fixed; (3) the normal displacement of the remaining two sides is zero. Boundary conditions of pore pressure: (1) the pore pressure of the node of the groundwater level is zero; (2) the bottom boundaries are impermeable

boundaries; (3) the four sides are impermeable boundaries. Input seismic waves excited in the slope direction for vibration, the seismic wave of the test is shown in Fig.9, and the peak acceleration is 0.198g. Fig.10 shows the comparison of the computational time history of the acceleration with the results in the model test in the upper part of the foundation and the slope crest.

It can be seen that the numerical results is slightly larger, the frequency of measured results is slightly higher due to the noise effect; but the computational results is integrally corresponding with that of the model test in the tendency and numerical value. Under earthquake effect, excess pore pressure in saturated sand increased significantly and the increase was obviously different in different parts. Fig. 11 shows the comparison of the computational time history of excess pore pressure with results of test in the typical parts of the slope, it can be seen the time history of excess pore pressure of computational results and the results in the model test are better according in the overall trend.

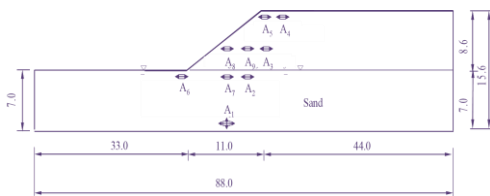


Fig.6 Position of accelerometer in slope (unit: m)

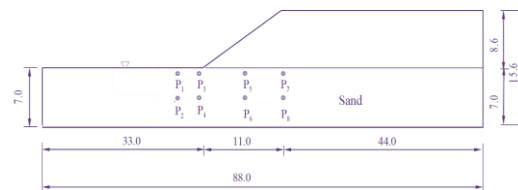


Fig.7 Pore pressure sensors in slope (unit: m)

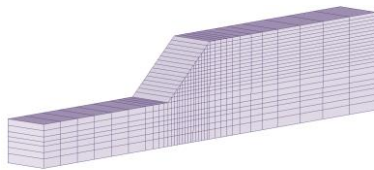


Fig.8 Finite element mesh

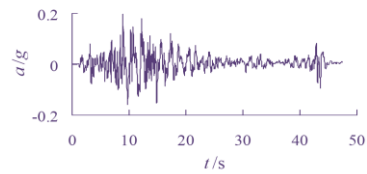
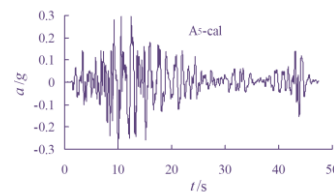
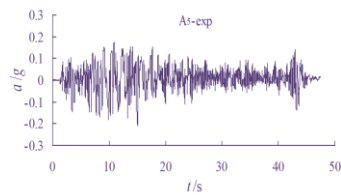
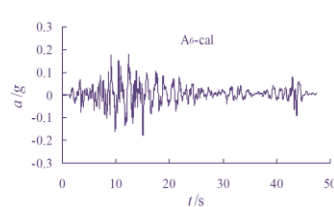
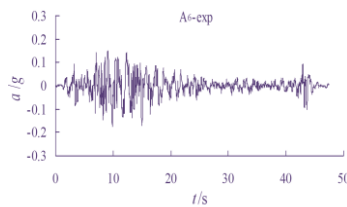


Fig.9 Input earthquake motion



(a) The accelerometer of A<sub>5</sub>



(b) The accelerometer of A<sub>6</sub>

Fig.10 In comparison with acceleration between test and computation

(a) The pore pressure gauge  $P_1$ (b) The pore pressure gauge  $P_3$ 

Fig.11 In comparison with excess pore pressure between test and computation

Fig.12 gives the distribution of the computational excess pore pressure of slope at 45s during earthquake. From the perspective of the distribution of pore pressure, it can be seen the horizontal soil pore pressure prior to the slope increased slightly and the pore pressure increased largely below the slope, the distribution trend inferred that the shallow saturated foundation had obvious liquefaction.

Fig.13 gives the distribution of computational horizontal displacement of slope at 45s during earthquake. It can be seen the displacement of horizontal saturated soil part and slope toe was larger, and the maximum values were 0.8 m and 1.0 m, while the local large deformation of saturated soil and slope toe led to the larger displacement of slope crest, the maximum value is about 1.0 m. These computational values showed the shallow saturated foundation had obvious liquefaction according to the displacement distribution of local large deformation.

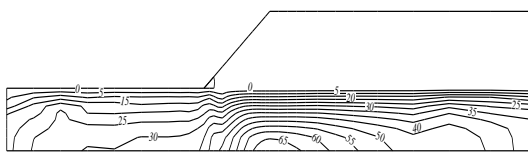


Fig.12 Contour of pore pressure at 45s(unit: kPa)

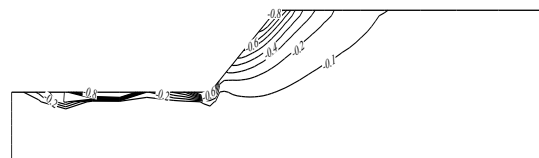


Fig.13 Contour of disp. at 45s(unit: m)

Analysis shows that there is an important influence of saturated soil liquefaction on the slope deformation. So the large displacements in slope bottom, slope toe and slope crest will have some adverse effects on the slope stability, it not only explains the failure phenomenon of slope, but also correspondingly explains the instability mechanism of slope.

#### 4. Conclusion

Throughout the comparison of the computational results with the experimental results, the saturated horizontal foundation liquefaction leads to the large displacement of slope toe, showing that the liquefaction of saturated horizontal foundation and the displacement of slope toe have a great impact upon the slope

stability. The dynamic coupled consolidation analysis reveals the causes and mechanism of sliding of slope because of the saturated horizontal foundation liquefaction under earthquake effect.

### References

- [1] Arulanandan K. Modeling lateral sliding of slope due to liquefaction of sand layer, *International Journal of Rock Mechanics and Mining Sciences and Geomechanics Abstracts*. Elsevier, 1996, 33(5): 227A-227A.
- [2] Nova-Roessig L, Sitar N. Centrifuge model studies of the seismic response of reinforced soil slopes. *Journal of geotechnical and geoenvironmental engineering*, 2006, 132(3): 388-400.
- [3] Kutter B L, Brandenberg S J, Singh P, et al. Pile foundations in liquefied and laterally spreading ground during earthquakes: centrifuge experiments & analyses. Center for Geotechnical Modeling, Department of Civil and Environmental Engineering, University of California, Davis, California, 2003.
- [4] Zienkiewicz O C, Shiomi T. Dynamic behaviour of saturated porous media; the generalized Biot formulation and its numerical solution. *International journal for numerical and analytical methods in geomechanics*, 1984, 8(1): 71-96.
- [5] Towhata I, Vargas-Monge W, Orense R P, et al. Shaking table tests on subgrade reaction of pipe embedded in sandy liquefied subsoil. *Soil Dynamics and Earthquake Engineering*, 1999, 18(5): 347-361.
- [6] Pastor M, Zienkiewicz O C, Chan A H C. Generalized plasticity and the modelling of soil behaviour. *International Journal for Numerical and Analytical Methods in Geomechanics*, 1990, 14(3): 151-190.
- [7] Chan A H C, Pastor M, Schrefler B A, et al. *Computational geomechanics*. Chichester: Wiley, 1999.
- [8] Liao S S C, Veneziano D, Whitman R V. Regression models for evaluating liquefaction probability. *Journal of Geotechnical Engineering*, 1988, 114(4): 389-411.